Free and Self-Trapped Charge-Transfer Excitons in Crystals of Dipolar Molecules of *N*,*N*-Dimethylaminobenzylidene 1,3-Indandione

S. Jursenas,*,†,‡ A. Gruodis,§ G. Kodis,‡ M. Chachisvilis,‡ V. Gulbinas,‡ E. A. Silinsh,|| and L. Valkunas‡,§

Institute of Materials Science and Applied Research, Vilnius University, Naugarduko 24, Vilnius 2006, Lithuania, Institute of Physics, A. Gostauto 12, Vilnius 2600, Lithuania, Department of General Physics and Spectroscopy, Vilnius University, Sauletekio 9, corp. 3, Vilnius 2054, Lithuania, and Institute of Physical Energetics, Latvian Academy of Sciences, Aizkraukles 21, LV-1006, Riga, Latvia

Received: June 16, 1997; In Final Form: November 5, 1997

In this paper we consider the spectral properties of exciton transitions of *N*,*N*-dimethylaminobenzylidene 1,3-indandione (DMABI) films and crystals, which are typical examples of polar molecular compounds. A large dipole moment in the electronic ground state and the considerable change (up to 12 D) of this value by excitation of a free DMABI molecule induce strong polarization of the surroundings, which causes the remarkable self-trapping effects in the crystal. The exciton−phonon coupling value $g = 1.87$ is estimated for the crystal. Charge-transfer (CT) exciton formation is observed in the absorption and luminescence spectra by analyzing the spectral behavior at various thicknesses of DMABI films. The CT excitons created along molecular stacks dominate in the spectra of the DMABI crystals. Coexistence of free and self-trapped CT excitons is discovered at elevated temperatures. The exciton band parameters are estimated, and the adiabatic energy potential energy for two self-trapped excitons is suggested. Relaxation paths of shallow short-lived and deeply trapped long-lived self-trapped CT excitons are discussed. Mechanisms of two-photon absorption and photoconductivity of DMABI crystals and films are considered.

1. Introduction

Exciton is a basic concept generally used by characterizing spectral properties of the electronic transitions in molecular crystals. Crystals of aromatic molecules, such as benzene, naphthalene, and anthracene, are classical examples demonstrating the excitonic origin of their optical spectra.[1−4] In the exciton theory approach, the molecular transition dipole moment is the main parameter that determines the excitonic feature of the spectrum. The presence of static molecular dipole moments in the ground and excited states evidently influences the strength of intermolecular interactions. According to the exciton theory, such static dipole moments cause an essential increase in the displacement (polarization) energy[2−4] and, moreover, stimulate strong exciton−phonon and/or exciton−vibrational mode interactions, which cannot be treated anymore as a small perturbation. The displacement (polarization) energy is responsible for the absorption band shift depending on the polarity of solvents or on the crystal structure, while the strong exciton−phonon interaction is mainly responsible for a distinct Stokes shift of the fluorescence band. Due to those interactions, the spectral properties of polar molecular systems are very sensitive to the changes in the structure and/or temperature variation, and strong optical nonlinear behavior might be observed.[5] Therefore, new possibilities for application of polar molecular films and crystals to nonlinear optics or molecular electronics are expected.[6−8]

The main objective of this paper is to study the excitonic transitions in organic molecular solids built up by dipolar molecules by various absorption and luminescence spectroscopy methods. The compounds under investigation are films and crystals of dipolar molecules of *N*,*N*-dimethylaminobenzylidene 1,3-indandione (DMABI). DMABI belongs to the polar derivatives of the 1,3-indandione consisting of two chromophoric fragments connected by the −CH═ bridge (Figure 1a). The molecule itself is almost flat due to strong π-electron conjugation, while the long axis of the donor (D) and acceptor (A) fragments are slightly tilted toward each other within the plane. Due to electron-donor and electron-acceptor properties of the DMAB and indandione fragments, respectively, an intramolecular electron transfer resulting in an asymmetric charge distribution takes place.[9,10] Quantum chemical calculations indicate a large dipole moment of the DMABI molecule being present in the ground state ($d_o = 2.3$ D) and a considerable change in this value in the excited state ($d_{ex} = 14.2$ D).[11] Such a giant change in the dipole moment of the molecule induced by the electronic transition should create a significant polarization in the surroundings, causing remarkable reorganization effects of the crystal lattice.

Let us briefly consider the crystal structure of DMABI. Similar to most polar carbocyclic and heterocyclic organic compounds, the DMABI crystals exhibit a well-expressed polymorphism. Depending on the conditions of crystal growth,[12] the DMABI compound may emerge in three crystalline modifications. Here we will discuss properties of the most stable α-modification. The single crystals of the α-modification are obtained from the solution as almost rectangular flakes (Figure 1b) of a dark red color up to $3 \times 4 \times 6$ mm^3 in size.[12] The crystal structures of the DMABI modifications are known.[9,12,13] The α-modification belongs to the monoclinic crystal system

† Institute of Materials Science and Applied Research, Vilnius University.
‡ Institute of Physics.
§ Department of General Physics and Spectroscopy, Vilnius University.
|| Latvian Academy of Sciences.

S1089-5647(97)01991-3 CCC: $15.00
Published on Web 01/22/1998

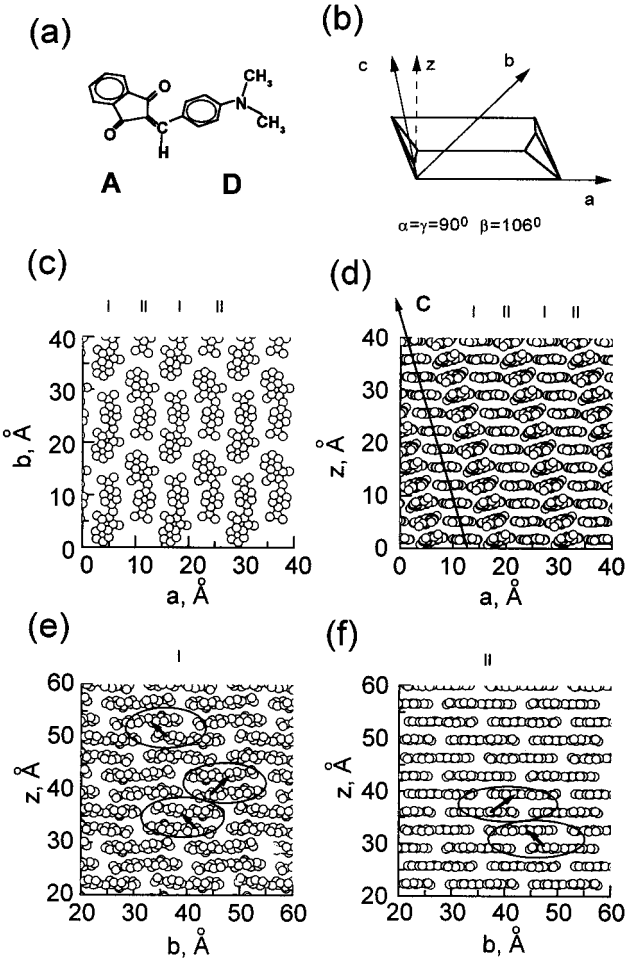

Figure 1. Crystal structure of the α-modification of the DMABI crystal for different crystal planes depicted from the X-ray diffraction data:[9] (a) DMABI molecule: A acceptor fragment and D donor fragment; (b) orientation of crystal axis, α, β and γ- corresponding angles; (c) molecular arrangement for the {001} crystal plane (points reflect the center position of C, O, and N atoms), I indicates molecules of the first type and II, those of the second type; (d) molecular arrangement for the {010} plane; (e) the type I molecular stack arrangement for the {100} plane, arrows indicate the possible intermolecular CT between D and A fragments; (f) the type II molecular stack arrangement for the {100} plane.

of the centrosymmetric space group $P2_1/c$.[9] According to X-ray diffraction data,[9] the crystal is built up by two types (I and II) of chemically identical DMABI molecules with a slightly different angle between donor and acceptor fragments of the molecules, i.e., 4.3° (I) and 8.0° (II), respectively. The lattice has eight molecules per unit cell arranged by four in two layers (see Figure 1c-f). All eight molecules are in nearly complanar orientation. Each of alternating layers is formed by the molecules of a single type differently packed in stacks (Figure 1e,f).

The stacked crystal structure created by alternating donor and acceptor fragments predetermines the possibility of the intermolecular charge-transfer (CT) state formation. Due to short interplane distances (3.3−3.5 Å) between the neighboring molecules in stacks, the optical transitions into the intermolecular charge-transfer states can be competitive with the intramolecular transitions.[9] The CT states can also be responsible for excellent photoconducting properties of DMABI crystals and films.[13]

In the present paper we consider formation of the excited states in vacuum-evaporated DMABI films and the bulk crystal. Utilizing various spectroscopic techniques, we identify transitions of free and self-trapped charge-transfer excitons. For DMABI crystal we estimate the exciton band parameters and the exciton−phonon coupling constant and suggest the potential energy diagram of exciton self-trapping process. On the basis of the energy diagram, we discuss the dynamics of shallow and deeply trapped excitons.

2. Materials and Methods

All samples have been prepared at the Institute of Physical Energetics in Riga. The DMABI compound was purified by gradient sublimation techniques according to ref 12. Vacuum-evaporated thin films of DMABI were obtained on glass or quartz substrates at room temperature and at $p = 10^{-5}$ Torr. The sublimation temperature of DMABI was 150 °C, the evaporation rate was about 10 Å/s, and the average thickness (d) was 0.125−1.9 μm. Single crystals of α-modification were grown from solution, according to a technique described in ref 12.

Absorption spectra of the films were obtained by the Beckman spectrophotometer (UV-5270).

Induced absorption spectra were measured by the absorption spectrometer, based on the passively mode-locked, feedback-controlled Nd:Glass laser (pulse duration 2 ps). The samples were excited by the basic radiation of the laser at 1.174 eV. Continuum light pulses generated in water provided the possibility to probe the induced absorption change within the 1.31−2.07 eV spectral range.

The steady-state luminescence was measured with the CW Ar^+ laser as the source for excitation (at 2.539 eV and output power 1 W). Luminescence spectra have been recorded by a spectrometer with a double monochromator (DFS-52) and a photomultiplier operating in the photon-counting regime. The polarized luminescence was obtained by CW excitation (at 2.539 eV) perpendicular to the sample plane. The luminescence was recorded in the backward geometry.

The luminescence kinetics was measured by the time-correlated single-photon-counting system. The excitation light source was a dye laser pumped by a mode-locked and frequency-doubled Nd^{3+}:YAG laser operating at 82-MHz repetition rate. The pulse repetition rate of the dye laser was reduced to 800 kHz by cavity dumping. The average energy of a single pulse was on the order of 10 nJ. Luminescence was detected by the cooled microchannel plate photomultiplier (Hamamatsu R2809U-05) using time-correlated single-photon counting. The fwhm of the instrumental response function was typically 60 ps, and the excitation photon energy was 2.294 eV.

The excitation intensity dependence of the luminescence spectra and the luminescence kinetics were also measured by a passively mode-locked YAG:Nd^{3+} laser based (pulse duration 30 ps) luminescence spectrometer. Time resolution (30 ps) was acheived by means of a CS_2 optical Kerr shutter. The first and the second harmonics of the laser were used for one-photon and two-photon excitation. The pumping density was varied from 1 to 500 MW/cm,[2] and the diameter of the excitation spot was about 1 mm. The spectral resolution was better than 5 meV.

Investigations were performed at room ($T = 298$ K) and liquid nitrogen ($T = 77$ K) temperatures.

3. Experimental Results

3.1. Absorption Spectra. The main absorption bands of DMABI compounds are located in the visible spectral region. Absorption spectra of DMABI films of different thickness (d), a powder of crystal of α-modification (the optical density of

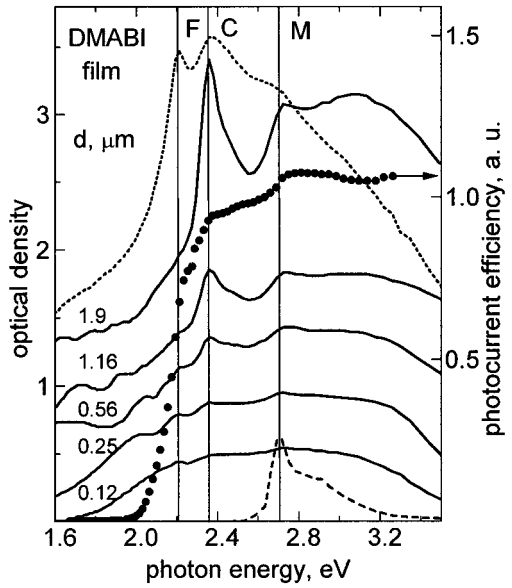

Figure 2. Absorption spectra of DMABI films of different thickness *d* (solid lines) on a quartz substrate, of DMABI solutions in *n*-heptane (dashed line), and of the DMABI crystal powder (dotted line). Points show the spectral dependence of the photocurrent efficiency measured for 1.16-μm DMABI film on a quartz substrate.

the bulk α-crystals was too high to be measured), and the DMABI solution in *n*-heptane (10^{-5} mol/L) are shown in Figure 2. The absorption spectra of DMABI solutions were analyzed in previous publications.[10,14] It has been shown that the spectrum can be divided into two groups of bands which are of different origin. The bands in the high-energy spectral region (maximum at 5.03 eV) correspond to the absorption of the indandione fragment of the molecule.[10] The visible band (M) (maximum at 2.71 eV) corresponds to the intramolecular absorption of the entire DMABI molecule.[10] Strong dependence of the absorption spectrum on the solvent polarity, indicating the dipolar character of the first singlet intramolecular transition, was also observed.[15]

The spectral position of the main absorption band (maximum at 2.71 eV) of the thinnest DMABI films coincides with the main absorption band (M) of the solution. By increasing the thickness of the film, the visible absorption band broadens and new solid-state absorption bands emerge. The main crystal-phase absorption band (C) of the thickest films ($d \geq 1$ μm) is located below the molecular band M, i.e. at 2.37 eV. This band also dominates in the spectrum of the powder of α-crystal. In addition to the C band, absorption spectra of DMABI films show a small peak (F) at 2.20 eV and an interference structure in the spectral region below 2.1 eV. Band F is clearly seen in the crystal spectrum. Absorption spectra of the DMABI films also show up as a broad band with the maximum at 3.1 eV above the molecular band M.

The F absorption band is weak in the film spectra, while its intensity increases when the absorption spectrum is monitored at some angle to the normal to the surface (Figure 3). This band is also considerably stronger in the absorption spectrum of the crystal powder (Figure 2), which closely resembles the film spectra. That is an indication that the dipole moment of the electronic transition, responsible for the F band, should be nearly perpendicular to the film surface. Thus, it seems that the vacuum-evaporated film contains microcrystals of the α-modification that grow along the *c*-axis (see Figure 1), the *ab*-plane being parallel to the substrate surface, however, randomly orientated. This situation is similar to the vacuum-deposited pyrene films.[16] The films possess a certain linear dichroism, which increases with the film thickness. In the spectrum of linear dichroism the optical transitions F and C are even more distinguished (Figure 3). The dichroism is probably caused by some degree of ordering of the microcrystals within a small area, created during the film fabrication.

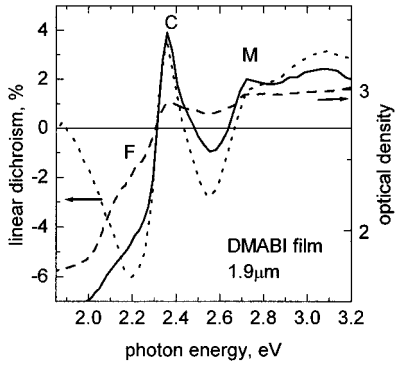

Figure 3. Spectral dependence of the linear dichroism for 1.9 μm DMABI film (dotted line) and absorption spectra obtained perpendicular to the film surface and by a 60° angle to the normal (solid and dashed lines, respectively).

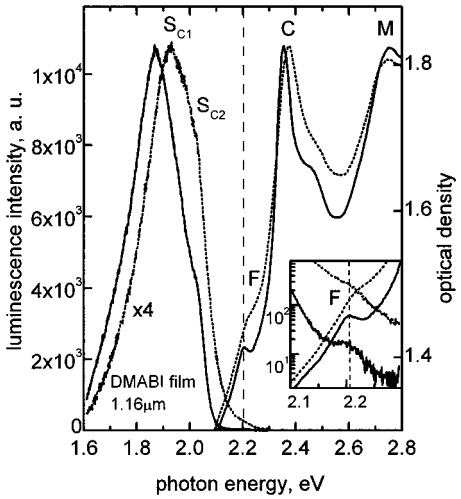

Figure 4. Absorption and luminescence spectra of the DMABI film ($d = 1.16$ μm) at $T = 298$ K and $T = 77$ K (dotted and solid lines, respectively). The inset depicts the enlarged region of the free exciton spectra.

Absorption spectra of the DMABI film ($d = 1.16$ μm) at different temperatures ($T = 298$ K and $T = 77$ K) are shown in Figure 4. The F and C absorption bands with decreasing temperature become narrower and shift to the lower energies; however, the spectral position of the M band is temperature-independent. The latter band also narrows and slightly increases in intensity by decreasing the temperature. A new absorption band at 2.45 eV manifests itself at $T = 77$ K.

Figure 5 depicts absorption spectra of the DMABI solution in *n*-heptane, the DMABI film ($d = 1.16$ μm), and the bulk crystal of the α-modification ($d = 2$ mm) recorded in the infrared (IR) spectral region. The DMABI films have a strong IR absorption (8000 cm^{-1} at 1.1 eV), which in our previous publications[11,15] was attributed to the CT excitons. However, the absence of this band in the crystal spectrum may be considered as strong evidence for reconsideration of this interpretation. The periodic lines in the IR spectra of the films can be attributed to the interference effects in the thin film on the low-energy edge of the absorption spectrum. The crystal spectrum shows only weak absorption lines ($\propto$10 cm^{-1}) in the

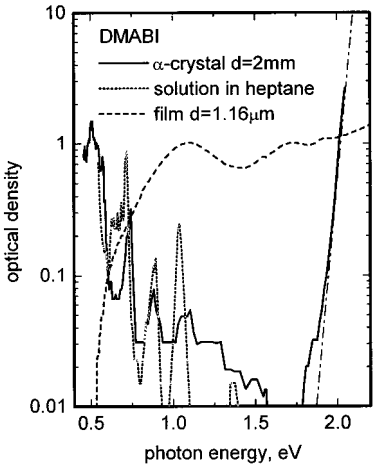

Figure 5. IR absorption of the DMABI α-crystal, the solution in heptane, and the film (solid, dotted, and dashed lines, respectively). The optical density of DMABI solution in heptane is multiplied by factor of 10^4 to compare the spectral positions and relative intensities of IR absorption bands.

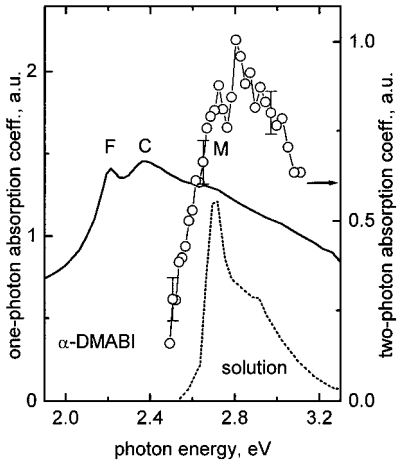

Figure 6. Comparison of the one-photon and two-photon absorption spectra of the DMABI crystal (solid line and points, respectively). The normalized spectrum of the DMABI solution in *n*-heptane is shown by the dotted line.

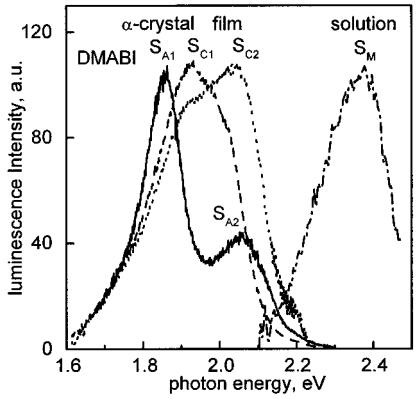

Figure 7. Normalized luminescence spectra of the DMABI crystal, films of $d = 1.9$ μm and $d = 0.25$ μm, and the solution in heptane (solid, dashed, dotted, and dashed−dotted lines, respectively).

far-IR spectral region probably caused by higher vibronic levels of the ground state of the DMABI molecule. This assumption is confirmed by the coincidence of the IR spectral lines of the DMABI crystal and the DMABI solution in *n*-heptane. The high-energy region of the crystal spectrum ($h\nu \geq 1.9$ eV) indicates a steep increase in the absorption due to the F and C bands, which correspond to the lowest energy electronic transitions in the DMABI solids.

3.2. Photocurrent Spectra. Typical spectral dependence of the photocurrent quantum efficiency of the DMABI film ($d = 1.16$ μm) on a quartz substrate is shown in Figure 2. The photocurrent quantum efficiency $\beta(h\nu)$ (amount of electrons per absorbed photon) has been measured in a sandwich type cell of the vacuum-evaporated DMABI film between Au and Al electrodes on a quartz substrate.

The photoconductivity threshold E_{th} coincides with the low-energy edge of the F absorption band. Since in that region $\beta(h\nu)$ can be described by the following empirical relation, $\beta(h\nu) = A(h\nu - E_{th})^{5/2}$, the E_{th} value can be defined via a linear relation[2] of $\beta^{5/2}$ on $h\nu$, giving $E_{th} = 1.95 \pm 0.02$ eV.[17]

3.3. Two-Photon Absorption Spectra. Excitation of the DMABI crystal by the high-intensity 2 ps duration light pulses at 1.174 eV induces the absorption of the sample in a transparent spectral region. Two kinds of intermediate states, i.e. virtual and real states, have been discovered in the DMABI crystal as being responsible for the two-photon absorption.[18] Although the 1.174-eV photon energy seems to be in an almost transparent spectral region of the DMABI crystal, more careful absorption measurements show weak absorption bands in the IR spectral range (from 0.8 to 1.5 eV) shown in Figure 5, which may be prescribed to higher vibrational levels of the electronic ground state of the DMABI molecule. The mean lifetime of this intermediate real state was estimated to be about 1 ps,[18] which is a typical value for excited vibrational states of large molecules.

During the two-photon absorption investigations, the energy of the first exciting photon was held constant at 1.174 eV, while the energy of the second photon was varied in the spectral range from 1.31 to 1.93 eV. As a result, a two-photon absorption spectrum emerged as a sum of excitation and probe light quanta in the spectral region from 2.48 to 3.10 eV (see Figure 6). The two-photon absorption is strong in the region of single-photon intramolecular absorption (band M with vibronic replicas), while the crystal-like F and C states, which dominate in the linear absorption spectrum, in the two-photon absorption are less active.

3.4. Luminescence Spectra. Room-temperature luminescence spectra of the DMABI solution in heptane, films, and crystal excited at 2.539 eV by CW Ar^+ laser are shown in Figure 7. The DMABI solution shows a broad Stokes-shifted (by 0.34 eV) luminescence (S_M) with the maximum at 2.38 eV. The crystal and films show the red-shifted luminescence at 1.7−2.05 eV. A broad luminescence band (S_{C2}) with the maximum at 2.04 eV is typical for thin DMABI films. By increasing the film thickness, a new S_{C1} luminescence band (at 1.92 eV) becomes dominant. It should be noted that the luminescence spectra of thick films could be slightly distorted by the reabsorption. The total luminescence intensity is enhanced more than 100 times by increasing the thickness of the film. This might be due to a smaller relative amount of the surface defects per unit volume for the larger microcrystallite. The luminescence spectrum of the α-modification crystal shows at least two characteristic bands dominating in the spectrum. The main luminescence band S_{A1} at 1.856 eV and a weaker luminescence band S_{A2} at 2.05 eV are evident. The Stokes shift of the S_{C1} luminescence band is 0.45 eV and 0.515 eV for S_{A1}. Both these bands are dominant in a wide range of excitation intensities.[19,20] At low-excitation conditions, the luminescence intensity of the DMABI crystals linearly increases with the excitation intensity, indicating the linear relaxation route, and saturates at high-

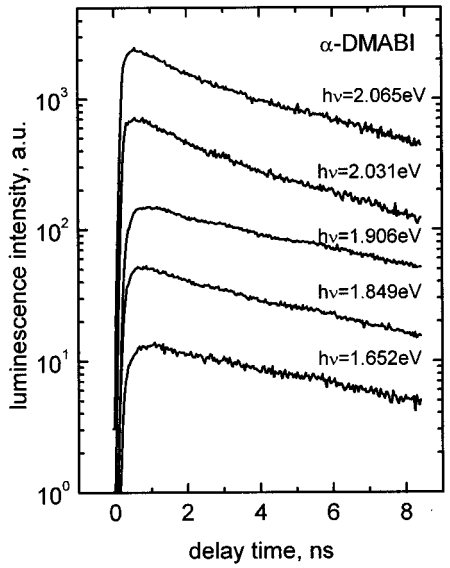

Figure 8. Luminescence kinetics of the DMABI crystal at different photon energies.

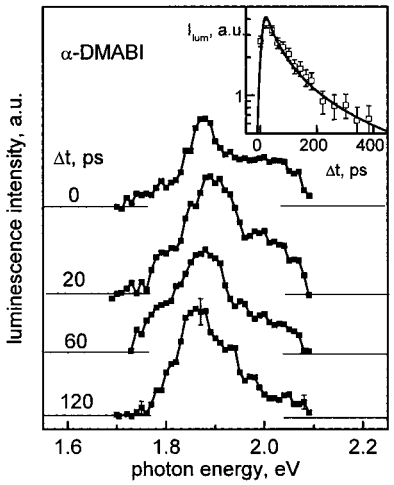

Figure 9. Time-resolved luminescence spectra of the DMABI crystal at high excitation intensities. The inset depicts the luminescence kinetics: points correspond to the experiment, lines to calculations according to eq 1.

intensity picosecond pulse excitation due to nonlinear relaxation. Only for the lowest excitation intensities could weak additional long-wavelength luminescence bands below the S_{A1} band be distinguished, which are probably caused by the lattice defects and impurities. This is in agreement with the density of local traps of 10^{17} cm^{-3} estimated in vacuum-evaporated DMABI films by means of thermally modulated space charge limited current.[21] It is to be noted that DMABI material shows good atmospheric stability and no remarkable photochemical changes in the luminescence spectra by laser irradiation. Similar luminescence spectra of fresh grown DMABI crystal (or fresh cut), measured after one year, were obtained.

Figure 4 shows the luminescence spectra of the DMABI film ($d = 1.16$ μm) at different temperatures, $T = 298$ K and $T = 77$ K. The total luminescence intensity increases by decreasing the temperature. The luminescence band S_{C1} shifts to lower energies by decreasing the temperature, in accordance with the shift of the C absorption band, while the band S_{C2} decreases in intensity in comparison with the S_{C1} band. Precise analysis of the high-energy side of the luminescence band indicates a weak luminescence band at 2.187 eV also being evident (see the inset in Figure 4). The energy position of this band coincides with the lowest crystal-like state F at 2.188 eV observed in the absorption. The spectral width at half-intensity of this resonant luminescence band is 40 meV, while the width of the S_{C1} band is 230 meV (for $T = 77$ K).

3.5. Luminescence Kinetics. The luminescence mean lifetime of DMABI solutions was found to range between several picoseconds and several tenths of picoseconds depending on solvent viscosity, while in a polymeric matrix the lifetime is about 1.5 ns (not shown). Isomerization processes in the excited state were determined as being responsible for the fast nonradiative relaxation of DMABI molecules in solutions and will be published elsewhere.

Luminescence kinetics of the α-modification DMABI crystals at low excitation intensities ($I = 20$ kW/cm^2, $h\nu_L = 2.294$ eV) for different photon energies is shown in Figure 8. The high-energy side of the luminescence spectra exhibits essentially nonexponential kinetics which contains a fast part with time constant $\tau_f = 800$ ps and a slow one with a time constant of 6 ns. At lower luminescence quantum energy the amplitude of the fast component decreases and the time dependence gradually transforms into a single-exponential kinetics. At the maximum of the spectra the lifetime of the S_{A1} state is $\tau_A = 7$ ns. For $h\nu < 1.85$ eV, this lifetime remains practically unchanged. The luminescence kinetics shows no changes by increasing the excitation intensity up to 10 times; nevertheless the kinetics is rather different at extremely high excitation intensities.

The time-resolved luminescence spectra of the crystal measured at 120 MW/cm^2 ($h\nu_L = 2.33$ eV, $\tau_L = 28$ ps) excitation intensity are presented in Figure 9. The inset depicts the time dependence of the total luminescence. During the excitation, two luminescence bands, S_{A2} and S_{A1}, evidently dominate in the spectra. The short-wavelength band S_{A2} rapidly decreases with time, and at time delay $\Delta t > 60$ ps only the main band, S_{A1}, remains. At high excitation intensities the nonlinear processes show up and the luminescence kinetics becomes nonexponential (see inset in Figure 9). The main channel of the nonlinear relaxation evidently is the singlet−singlet fusion.[1] By solving a corresponding kinetic equation for excitons,

$$\frac{dn}{dt} = G(t) - \gamma n^2 - \frac{n}{\tau} \qquad (1)$$

the temporal evolution of the spectral-integrated luminescence ($I_{LUM}(t) \propto n(t)$) can be obtained. Here the first term on the right-hand side of eq 1 is the generation rate, and the subsequent terms are recombination rates for bimolecular and linear processes, respectively. To describe the luminescence kinetics at high excitation intensities, the linear excitation decay value for S_{A1}, $\tau_A = 7$ ns, obtained from the low excitation measurements (Figure 8) and the absorption constant $a = 2 \times 10^4$ cm^{-1} measured for thick films (Figure 2) have been used. The best fit (inset in Figure 9) of the single free parameter which is the value of the bimolecular annihilation rate constant gives $\gamma = 5 \times 10^{-10}$ cm^3/s. The rapid luminescence ($\tau < 3 \times 10^{-11}$ s) from the S_{A2} state in the α-crystals is neglected in the analysis of the luminescence kinetics. The excited state S_{A2} is short-lived in comparison to the S_{A1} state and is observable in luminescence during the excitation pulses action only. It may be assumed that bimolecular recombination of S_{A2} excited states is much more efficient compared with the S_{A1} states.

3.6. Polarization Peculiarities of Luminescence. Polarization of the luminescence spectra of the thin DMABI film is weak and independent of the polarization of the excitation light, while it depends on the film orientation. It has been determined

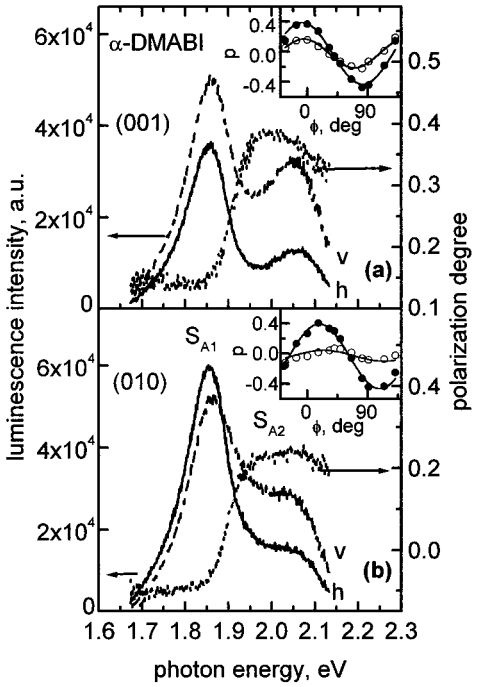

Figure 10. Polarized luminescence spectra of the DMABI crystal monitored at different crystal planes. Directions of polarized luminescence are horizontal (solid line) and vertical (dashed line); the dotted line indicates the spectral dependence of the polarization degree. Angular dependencies of the luminescence polarization degree for the two self-trapped exciton bands are depicted in the insets (solid points correspond to the S_{A2} band, open points to S_{A1}).

that the luminescence polarization as well as the linear dichroism is caused by a particular orientation of microcrystals. The degree of polarization of the luminescence obtained as

$$p = \frac{I_v - I_h}{I_v + I_h} \tag{2}$$

is less than 0.05 in the whole spectral region. Here I_v and I_h are vertical and horizontal components of the luminescence, respectively.

Figure 10 presents the polarized luminescence spectra of the DMABI crystal as well as the corresponding crystal planes {001} and {010} of the excitation/recording, which coincide with molecular arrangement projections shown in Figure 1c,d (unfortunately, due to the growth of the crystal, there are no possibilities to get similar data from the {100} crystal plane, as it is shown in Figure 1e,f). The S_{A1} and S_{A2} luminescence bands possess different polarization degree. The largest polarization degree corresponds to the high-energy luminescence band S_{A2} ($p = 0.4$) (see Figure 10a). For the spectral region of the main luminescence band S_{A1} the polarization decreases to $p = 0.1$, with a further gradual decrease toward the lower energy wing. The same features of the polarized luminescence are found in other crystal configurations. It should be noted that the spectral dependence of the polarization degree of the crystal is also independent of the excitation light polarization.

By analyzing the dependence of the luminescence polarization degree on the rotation angle (φ) of the analyser (e.g., this rotation by 90° changes the horizontal component of the luminescence vertical), the orientation of the corresponding optical-transition dipole moment projection on the crystal plane can be determined. These angular dependencies of the polarization degree at the peak positions of the S_{A1} and S_{A2} luminescence bands are shown in the insets of Figure 10. For the {001} crystal plane, the maximum of the polarization degree is found at $\varphi = -3°$. This can be explained by assuming that the dipole moment of the S_{A1} and S_{A2} optical transitions are orientated almost along the *b*-crystal axis. For the {010} crystal plane, the maximum of the polarization degree is found at $\varphi = 18°$. This is consistent with the orientation of the stack axis *c*, which, according to the crystallographic data[9], forms a 106° angle to the *a*-crystal axis (see Figure 1b,d).

4. Discussion

There are several arguments supporting the assignment of the lowest energy absorption components (bands F and C) to the transitions into the *intermolecular* CT states, while the band M is assigned to the *intramolecular* transition. It is known that in crystals composed by donor and acceptor molecules alternating in quasi-one-dimensional arrays the CT complexes can give rise to new optical transitions in the visible spectral range, where the individual donor and acceptor molecules do not absorb.[1,2]

In crystals, flat DMABI molecules are packed face-to-face, creating molecular stacks with 3.5-Å interplane distances (Figure 1d). The polar D and A fragments of the molecules are packed in an alternating sequence to optimize the Coulomb interaction. At distances less than 3.5 Å the electron clouds of planar aromatic molecules overlap in face-to-face orientation, and electron exchange interactions can become significant.[22,23] Correspondence of the F and C absorption bands to the *intermolecular* CT transitions is confirmed by the photocurrent quantum efficiency $\beta(h\nu)$ spectra (see Figure 2). The intermolecular CT origin of F and C transitions is also in line with the dependence of the photocurrent quantum efficiency on the external magnetic field.[24] That also implies that the photogeneration of free charge carriers in DMABI crystals and films actually occurs via intermolecular charge-transfer states and is of intrinsic nature. Consequently, the $E_{th} = 1.95$ eV may be regarded as an actual energy gap E_G of the crystal. This situation is rather extraordinary for organic molecular solids.[2] Usually the first singlet transition is situated below the energy gap E_G. In case of DMABI the E_G value is not only below the intramolecular M band but also below the intermolecular CT band (i.e., F band) and practically coincides with the S_{1C} band at 1.92 eV (see Figure 7). This extraordinary effect may be explained by the high polarity of the DMABI molecule and considerable intermolecular interaction.

The dissociation of intermolecular CT states and formation of free charge carriers in polar media should occur with a high probability. It explains the reported high photosensitivity of the DMABI crystals and films[10,13] (the ratio of the photocurrent to the dark current has been found to be on the order of 10^4-10^5). It is noteworthy that the crystals of the α-modification[13] where the stacked structure is the most clearly expressed possess the largest photocurrent effect.

Therefore, the relative increase in the intensity of F and C absorption bands compared to the M band by increasing the thickness of the film (Figure 2) could be related to the manifestation of the intermolecular CT states or some hybridized Frenkel−CT exciton states.[25]

The intermolecular character of the F and C bands is in line with the blue shift of these bands by increasing the temperature (Figure 4); that is, a temperature increase from 77 to 298 K causes a blue shift of the F and C bands up to 15 meV, while the M band, being due to the intramolecular absorption, shows no shift at all. This is consistent with the fact that the CT exciton binding energy decreases by increasing the intermolecular distance[26] because of the thermal expansion of the lattice.

The difference in origin of the molecular absorption band M and the crystal absorption bands F and C is also evident from the comparison of the two-photon and one-photon absorption spectra (Figure 6). The M band is present in both the one-photon and two-photon absorption spectra, while the F and C bands manifest themselves only in one-photon absorption. These peculiarities of the absorption could be explained on the basis symmetry of the system. A change in the parity between the initial and final states is required for every photon involved in the transitions (in the dipole approximation). Thus one- and two-photon transitions require different parities of the final states.[27] For molecules without the center of inversion, as for the DMABI molecule, in general, each state is of mixed parity, and consequently, transitions between all electronic states involving any number of photons are symmetry-allowed. Thus, all molecular states (the M state in our particular case) can be observed in both the linear and two-photon absorption spectra. The intermolecular CT transition states F and C have higher symmetry determined by the symmetry of the crystal and, consequently, have more strict selection rules. According to these selection rules, a centrosymmetric crystal like DMABI[9] should be inactive in two-photon absorption and second-harmonic generation.[27]

However, it has been demonstrated[28] that *intermolecular* charge transfer contributes to the second-order susceptibility in centrosymmetric systems, although this selection rule is not strict and may allow two-photon absorption and second-harmonic generation in the case of intermolecular CT transitions. Thus, both the two-photon absorption via a virtual state and two-step absorption via a real intermediate state might be observed. In our case the two-photon absorption actually occurs in the intermolecular CT band at about 2.3 eV, and since the two-photon absorption overlaps with the second-harmonic generation, this effect is supposed to enhance considerably the nonlinear anti-Stokes luminescence in accordance with experimental data.[5,11]

The static dipole moment of the DMABI molecule is present both in the electronic ground and in the excited states, and the extremely dipolar nature of the CT exciton itself implies the existence of strong intermolecular Coulomb forces, which can create pronounced changes in the geometry after the exciton generation. Strong local lattice deformation, leading to a strong exciton−phonon coupling and, thus, to polaronic effects, might be expected.[29] The exciton−phonon coupling value g is often used to characterize the exciton−phonon coupling strength and the depth of exciton self-trapping (E_{ST}).[2,30,31] This parameter reflects the ratio of the lattice relaxation energy (E_{LR}) to the half exciton bandwidth (B) and determines a criterion for self-trapped exciton formation.

The exciton−phonon coupling value may be estimated from the steepness parameter σ of the Urbach−Martienseen rule:

$$A(E) = A(E_0)\exp\left(-\sigma\frac{E_0 - E}{k_B T}\right) \qquad (3)$$

where T is the lattice temperature, k_B is the Boltzmann constant, E_0 is the converging energy, and $A(E_0)$ is the absorption coefficient at E_0. For high temperatures and assuming that the low-energy lattice phonons are active in the long-range interaction, the exciton−phonon coupling constant is inversely proportional to σ, namely, $g = s/\sigma$,[32] where s is the steepness index ($s = 1.5$ for three-dimensional systems[33]). At room temperature the Urbach edge of the absorption spectrum of the DMABI crystal under consideration (Figure 5) gives the value $\sigma = 0.8$,

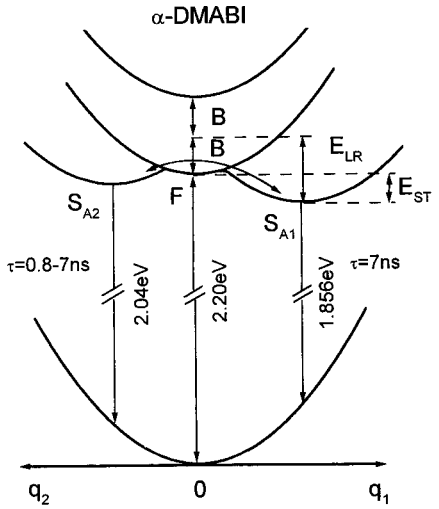

Figure 11. Potential energy scheme of two different self-trapped CT excitons in the DMABI crystal of α-modification.

which is actually slightly less than the high-temperature-limit value. The estimated exciton−phonon coupling constant $g = 1.87^{+0.05}_{-0.29}$ is larger than unity, indicating that self-trapped excitons should have lower energy. The obtained large g value and a short 3.5 Å average distance between the nearest molecular planes in a crystal make the DMABI similar to pyrene, β-dichloranthracene, or α-perylene organic crystals, where strong self-trapping effects were observed.[34] The excitation kinetics for such systems (where the exciton−phonon interaction is strong) is in general rather complex. Initially after the optical generation, the exciton may be delocalized and behaves like a wave spreading through the crystal. However, due to strong interaction, the exciton becomes localized and can be self-trapped in the potential well associated with the local lattice distortion induced by the exciton itself.[30,31] Typical examples of organic materials where the exciton−phonon coupling is strong are pyrene crystals, which possess a double-well potential in the excited state,[16,34,35] and the anthracene−PMDA (pyromellitic acid dianhydride) crystals, where a quasi-one-dimensional case of the CT exciton self-trapping takes place.[22] The free and self-trapped excitons were simultaneously observed in these organic systems.

The luminescence and absorption spectra of the DMABI film presented in Figure 4 demonstrate a typical picture of coexistence of the free and self-trapped excitons. A broad Gaussian band S_{C1} (at 1.92 eV) with a significant Stokes shift (0.43 eV) dominates in the luminescence spectra. A weak narrow 0−0 optical transition at 2.187 eV in the high-energy wing of this band can be distinguished, which is in resonance with the corresponding narrow absorption line. The spectral width at half-intensity of this resonant luminescence line is 40 meV, while the width of the S_{C1} bands is 230 meV (for $T = 77$ K). Coexistence of the free and self-trapped excitons at room temperature can be explained by the thermal activation of the free exciton state across an activation barrier (see Figure 11).

The measurements of the luminescence kinetics (Figure 8) yield lifetimes of 0.8−7 ns, which are typical values for singlet excitons. The relaxation from the self-trapped exciton states is the main luminescence route for all DMABI compounds in a wide range of excitation intensities.[19] Only for the highest excitation intensity ($I = 120$ MW/cm^2) does the onset of bimolecular exciton reaction take place with the rate constant $\gamma = 5 \times 10^{-10}$ cm^3/s for the α-modification of the crystal.

The dynamics between two self-trapped exciton luminescence bands S_{C1} and S_{C2} observed by increasing the thickness of the

film can be related to the intermolecular charge transfer which is the most pronounced in the crystal structure. By increasing the thickness of the film, the intensity of the self-trapped exciton luminescence S_{C1} as well as the Stokes shift of this band increases. Meanwhile, formation of new CT states (F and C) in the absorption spectra is seen (Figure 2). The crystal luminescence band S_{A1} has the largest Stokes shift, while the lowest absorption bands F and C are situated at the same energy for the crystal and for the films of different thickness. That is, probably, due to the enhancement of the self-trapping of CT excitons by formation of the crystal structure, because of the long-range origin of the CT−exciton coupling to the lattice phonons.

The luminescence spectra of the α-crystal reflect the competition between two self-trapped exciton bands as well. These two luminescence bands are of different degrees of polarization. The polarization properties can be explained by assuming that the observed luminescence is due to intermolecular charge transfer along the D−A molecular stack. Nearly complanar orientation of all molecules in the DMABI α-crystal simplifies the analysis. The dipole moment of the intramolecular transition should be orientated along the D−A axis of the molecule (*b*-axis of the crystal). However, the dipole moment of the self-trapped exciton transition is found to be orientated along the *c*-axis of the crystal. This indicates that intermolecular CT within the molecular stack takes place. Possible transitions into the CT states are indicated in Figure 1 by arrows. Two types of CT complexes could be distinguished: the "dimerlike" structures, formed by the antiparallel-orientated molecules of type I (Figure 1e), and the "steplike" structures characteristic for both molecular layers (Figure 1e,f).

Two-band self-trapped exciton luminescence dynamics has been observed also in other dimeric organic crystals such as pyrene or perylene. The self-trapped exciton states there are named as excimers.[36] These excimer states are not as polar as charge-transfer excitons since identical moieties (i.e., the donor and acceptor molecules are identical) are involved. In pyrene and perylene, besides the main deeply trapped excimer states, the shallow short-lived metastable state was also observed.[16,37,38] The intermediate self-trapped exciton luminescence in pyrene was found to be weakly Stokes-shifted with respect to the monomer luminescence in solution. However, the shallow self-trapped exciton band of the DMABI crystal is strongly shifted in comparison with the monomer luminescence in the neutral solvent (see Figure 7). This might be due to the nonzero dipole moment of the DMABI molecule and the CT origin of the transition. Since in the dimer structures the intermolecular CT occurs between the D and A fragments of two DMABI molecules and formation of the intermolecular CT state is accompanied by a local deformation of the lattice (a decrease of the intermolecular distance of the dimer), this state may be actually regarded as the real CT excimer state. The CT in the "steplike" structure occurs between identical molecules; however, this situation is more similar to the charge-transfer excitons observed in weak CT donor−acceptor crystals such as anthracene−PMDA.[22] Calculations of geometrical and energy parameters of the CT excimer by means of the atom−atom potential and Coulombic interaction approaches or by molecular dynamics techniques might be useful for further investigations of these systems.

By another explanation the two self-trapped exciton bands present in these DMABI compounds could be attributed to the different molecular stacks of type I and type II molecules. In that case it could be assumed that the molecules of type I, forming dimer structures in the molecular stack, give the long-lived highly localized self-trapped exciton band S_{A1}, while the type II molecular stack gives the short-lived S_{A2} excited state.

The potential energy scheme that can be applied by describing the spectroscopic properties of the DMABI crystal of the α-modification is shown in Figure 11. Here, two configurational coordinates q_1 and q_2 are attributed to the S_{A1} and S_{A2} states, respectively. The population in the high-energy band S_{A2} shows a two-component decay with 800-ps and 7-ns relaxation times. The long component is close to that observed for the low-energy band S_{A1}. This allows us to assume that for some delay time after the excitation both self-trapped exciton states are in thermal equilibrium and the excited state S_{A2} is thermally activated from the S_{A1} across a small (on the order of k_BT) activation barrier, as shown in Figure 11 by the arrow. One should indicate that there is no need to cross the point $q_1 = q_2 = 0$. Unfortunately, it is difficult to distinguish a small increase in the S_{A1} luminescence caused by the short-lived component of S_{A2} luminescence. Therefore, it is difficult to distinguish either that the S_{A2} excited state is initially occupied or that the bypass in the energy relaxation takes place,[37] and both S_{A1} and S_{A2} excited states are occupied simultaneously after a short pulse excitation. By decreasing the temperature, the luminescence of the shallow trapped excitons decreases, while that of the deeply trapped excitons increases. This indicates that a small part of excitation overcomes the activation barrier from the S_{A1} to the S_{A2} excited state at low temperature.

This explanation is in agreement with the estimations of the self-trapping energy of the system. The Stokes shift of the self-trapped exciton luminescence with respect to the free exciton state equals[30] $\Delta h\nu = 2E_{LR} - B$ (as shown in Figure 11). Knowing that $g \equiv E_{LR}/B$, the self-trapping energy $E_{ST} = E_{LR} - B$ may be estimated. This estimation is correct in terms of the Franck−Condon approximation, and at low temperature, however, we use this relation between the exciton−phonon system parameters with some reservations, as the first rough approximation. If we assume that the excitons from the F state are localized at the S_{A1} excited state with the estimated exciton−phonon coupling constant $g = 1.87$, then the exciton band parameters are $B = 0.125$ eV, $E_{LR} = 0.235$ eV, and $E_{ST} = 0.11$ eV. Another, less possible, assumption is that the excitons from the F state are localized at the S_{A2} excited state, then $B = 0.055$ eV, $E_{LR} = 0.102$ eV, and $E_{ST} = 0.047$ eV. In both cases E_{ST} is found to be equal to several k_BT. At room temperature occupation of the free exciton state and of the shallow partially delocalized self-trapped exciton state S_{A2} is relatively long-lived due to their additional population by thermal activation of long-lived deeply self-trapped S_{A1} excitons. To get a more detailed diagram of the exciton self-trapping process with corresponding thermal activation barrier energies, a careful analysis of the time-resolved luminescence spectra dependence on the temperature is needed. This will be one of our future objectives of the studies of the excitons in the DMABI crystals.

5. Conclusions

The DMABI crystal is a typical example of polar organic crystals,[2] i.e. built up by dipolar molecules where molecules are bound in the crystal by van der Waals and Coulomb forces. A large dipole moment of the free DMABI molecule in the ground state and essential change of this value after the electronic transition into a higher state induce a significant polarization effect of the surroundings in the crystal structure, evidently causing the remarkable self-trapping effects. At room temperature the exciton−phonon coupling value $g = 1.87$ was

estimated for the crystal. The coexistence of free and self-trapped excitons was observed in this strong exciton−phonon-coupled system at elevated temperatures. The exciton bandwidth $B = 0.125$ eV and the lattice relaxation energy $E_{LR} = 0.235$ eV are estimated for the DMABI crystal of the α-modification. It is noteworthy that a specific dynamics of deep and shallow self-trapped exciton luminescence, similar to that of the excimers in dimeric pyrene and perylene crystals, is evident in the polar DMABI crystal. This might be due to a few-step self-trapped exciton formation, which is a characteristic feature of the strong exciton−phonon-coupled dimeric system.

The DMABI molecules are arranged in the crystal as a stacked structure to optimize the polar interaction between the flat D and A fragments. The charge transfer within the stack causes excellent photocondoctivity of DMABI crystals and films. The singlet CT excited states manifest themselves in the optical absorption and luminescence spectra. The compounds under consideration could be attributed to the weak CT organic crystals. The intermolecular charge transfer is similar to the transitions observed in mixed stacked DA CT complexes;[1,22] however, the donor and acceptor fragments in DMABI are situated in the same molecule. Therefore, the CT transition within the stack should cause significant intramolecular charge redistribution, which changes the dipole moment of the molecule and leads to considerable polarization of the crystal surroundings. It could be expected that such mixed inter−intramolecular CT excitons could show a two-dimensional feature within the same molecular stack.

Acknowledgment. This research was supported by Joint Grant ISF-Lithuanian Government No. LH6100 and by the Lithuanian State Foundation of Science and Studies Grant No. 96-300/2F. We thank I. Kaulach for photocurrent measurements and for stimulating discussions.

References and Notes

(1) Pope, M.; Swenberg, C.M. *Electronic Processes in Organic Crystals*; Oxford: New York, 1982; Chapter 1.
(2) Silinsh, E. A.; Capek, V. *Organic Molecular Crystals. Interaction, Localization and Transport Phenomena*; AIP Press: New York, 1994.
(3) Agranovich, V. M. *Exciton Theory;* Nauka: Moscow, 1968 (in Russian).
(4) Davydov, A. S. *Theory of Molecular Excitons;* New York: Plenum Press, 1971.
(5) Gailis, A. K.; Kolesnikov, V. A.; Silinsh, E. A. *Izv. Akad. Nauk Latv. SSR, Ser. Fiz. Tekh. Nauk* **1978**, *1*, 20.
(6) Bosshard, C. *Adv. Mater.* **1996**, *8*, 385.
(7) Serbutoviez, C.; Bosshard, C.; Knöpfe, G.; Wyss, P.; Pretre, P.; Günter, P.; Schenk, K.; Chapuis, G. *Chem. Mater.* **1995**, *7*, 1198.
(8) Rutkis, M. A.; Wistus, E.; Lindquist, S. E.; Mukhtar, E.; Liberts, G.; Zauls, V. A.; Klimkans, A. B.; Silinsh, E. A. *Adv. Mater. Opt. Electron.* **1996**, *6*, 39.
(9) Magomedova, N. S.; Zvonkova, Z. V. *Kristallography* **1978**, *23*, 281 (in Russian).
(10) Dimond, N. A.; Mukherjee, T. K. *Discuss. Faraday Soc.* **1971**, *51*, 102.
(11) Valkunas, L.; Juodzbalis, D.; Urbas, A.; Gruodis, A.; Durandin, A.; Silinsh, E. A.; Klimkans, A.; Larssons, S. *Adv. Mater. Opt. Electron.* **1993**, *3*, 221.
(12) Aleksandrov, S. B.; Meiyere, G. F.; Yurel, S. P. *Organic Semiconductor Materials*, 3rd ed.; Perm University, 1980; Chapter 1 (in Russian).
(13) Magomedova, N. S.; Kolninov, O. V.; Ruchadze, Y. G.; Zvonkova, Z. V. *Zh. Fiz. Khim.* **1975**, *49*, 1322 (in Russian).
(14) Weiler Feilhenhold, H.; Lowenstein, R. M. J.; Agranat, J.; Bergmann, E. D. *Isr. J. Chem.* **1969**, *7*, 99.
(15) Valkunas, L.; Gruodis, A.; Juodzbalis, D.; Urbas, A. *Mol. Cryst. Liq. Cryst.* **1993**, *230*, 163.
(16) Seyfang, R.; Port, H. Fischer, P.; Wolf, H. C. *J. Lumin.* **1992**, *51*, 197.
(17) Jursenas, S.; Gruodis, A.; Kodis, G.; Valkunas, V.; Kaulach, I.; Silinsh, E. A. In *Optical Organic and Semiconductor Inorganic Materials*; Silinsh, E., Medvids, A., Lusis, A., Ozols, A., Eds.; SPIE Proceedings Series; 1997; Vol. 2968, p 24.
(18) Gulbinas, V.; Kodis, G.; Valkunas, V. *J. Phys. Chem.* **1996,** *100*, 19441.
(19) Jursenas, S.; Gruodis, A.; Kodis, G.; Chachisvilis, M.; Valkunas, L. *Lith. J. Phys.* **1994**, *34*, 222.
(20) Jursenas, S; Gruodis, A.; Kodis, G.; Chachisvilis, M.; Valkunas, L. In *Fast Elementary Processes in Chemical and Biological Systems*; Tramer, A., Ed.; AIP: Woodbury, New York, 1996; p 191.
(21) Muzikante, I.; Fonavs, E.; Silinsh, E. A. *Adv. Mater. Opt. Electron.* **1996**, *6*, 283.
(22) Harrer, D.; Pilpott, M.R. In *Spectroscopy and Excitation Dynamics of Condensed Molecular Systems*; Agranivich, V. M.; Hochstrasser, R.M., Eds.; Amsterdam: North Holland, 1983; p 27.
(23) Bulovic, V.; Burrows, P. E.; Forrest, S. R.; Cronin, J. A.; Thompson, M. E. *Chem. Phys.* **1996**, *210*, 1.
(24) Kaulach, I.; Silinsh, E. A. *Latvian J. Phys. Technol. Sci.*, in press.
(25) Rossi, L.; Bongiovanni, G.; Kalinowski, J.; Lanzani, G.; Mura, A.; Tubino, R. *Chem. Phys Lett.* **1996**, *257*, 545.
(26) Czekalla, J.; Breigleb, G.; Herre, W.; Reed, C.; *Z. Electrochem.* **1959**, *63*, 1157 (in German).
(27) Stegeman, G. I.; Cha, M.; Lawrence, B. L.; Torruellas, W. E.; Baker, G. In *Photoactive Organic Materials*; Kajzar, F., Agranovich, V. M., Lee, C. Y. C., Eds.; Kluwer Academic Publishers: Dordrecht, 1996; p 75.
(28) Ashwell, G. J.; Lesson, P. In *Electrical and Related Properties of Organic Solids*; Munn, R. W., Miniewicz, A., Kuchta, B., Eds.; Kluwer Academic Publishers: Dordrecht, 1997; p 297.
(29) Jursenas, S.; Gruodis, A.; Kodis, G.; Valkunas, L. *Adv. Mater. Opt. Electron.* **1996**, *6*, 387.
(30) Toyozawa, Y. In *Organic Molecular Aggregates*; Reineker, P., Haken, H., Wolf, H. C., Eds.; Springer: Berlin, 1983; p 90.
(31) Rashba, E. I. In *Excitons*; Rashba, E. I., Sturge, M. D., Eds.; North-Holland: Amsterdam, 1982.
(32) Matsui, A.; Mizuno, K.; Iemura, M. *J. Phys. Soc. Jpn.* **1982**, *51*, 1871.
(33) Schreiber, M.; Toyozawa, Y. *J. Phys. Soc. Jpn.* **1982**, *51*, 1544.
(34) Matsui, A. H. In *Self-Trapped Excitons*; Song, K. S., Williams, R. T., Eds.; Springer: Berlin, 1993; p 300.
(35) Matsui, A. H. *Pure Appl. Chem.* **1995**, *67*, 429.
(36) Birks, J. B. *Rep. Prog. Phys.* **1975**, *38*, 903.
(37) Matsui, A. H.; Nakamura, T.; Natakani, S.; Ohno, T.; Mizuno, K. *Synth. Met.* **1994**, *64*, 177.
(38) Sumi, H. *Chem. Phys.* **1989**, *130*, 433.